Memorandum

November 16, 2021 (revised 31st Jan. 2022, 7th Apr. 2022)

TO: WECC Modeling and Validation Subcommittee (MVS) and Renewable Energy Modeling Working Group (REMWG)

FROM: Deepak Ramasubramanian, EPRI; dramasubramanian@epri.com
CC: Anish Gaikwad, Evangelos Farantatos, EPRI; Brian Johnson, UW; Sairaj Dhople, UMN; Olaoluwapo Ajala, Alejandro Dominguez-Garcia, UIUC; Pouyan Pourbeik, PEACE®

SUBJECT: **PROPOSAL FOR SUITE OF GENERIC GRID FORMING (GFM) POSITIVE SEQUENCE MODELS**

This document describes a proposal for generic positive-sequence stability models for the most popular forms of grid forming (GFM) inverters (used for coupling inverter-based resources to the power grid). The development of this suite of models is based on research work carried jointly across EPRI, University of Washington (UW), University of Illinois Urbana Champaign (UIUC), and University of Minnesota (UMN). Associated research results and further details are available in references [1] [2] [3] [4] [5].

The suite of generic GFM models can represent, in a general way, three different types of GFM control methods that have been proposed in the literature. These methods are:

1. Droop based GFM
2. Virtual Synchronous Machine (VSM) based GFM
3. Dispatchable Virtual Oscillator (dVOC) based GFM

It should be understood, that at present, the proposed positive sequence grid forming generic models (across WECC MVS) are based on research and are generic in nature and do not necessarily represent any actual equipment being offered by equipment vendors, nor should it be construed that such offerings are available at present from all vendors.

An underlying structural similarity across these three methods [1] [2] forms the basis for this suite of generic models. Further, previous research work [4] [5] [6] has also uncovered an operational similarity with the use of a phase locked loop (PLL) based generic model. As the dynamic behavior of this PLL based generic model can be represented using the existing REGC_C+REEC_D+REPC_A generic models, the model specifications of these models are not provided in this document and instead only its performance is shown. In the following sections, the specifications of the suite of models along with its parameters will first be provided followed by testing and validation results.

Finally, note that in a previous version of this memo [7], a single model was proposed which could be parameterized appropriately such that it could represent all three (3) structurers presented here in addition to the structure that is similar to the combination of REGC_C+REEC_D+REPC_A models. When this was presented at the January, 2022 WECC MVS meeting there was quite favorable feedback by all stakeholders, however, one constructive feedback offered was to split the model into three (3) distinct models to represent the three (3) different control-strategies for an easier model user experience. Hence the revision here to offer the three (3) distinct model structures. Additionally, although active and reactive power limits can be handled by a back-end plant controller model (such as REPC_C) a suggestion was made to include these active power and reactive power limits within the model itself. As a result, the revised model specifications include an active and reactive power limit logic, whose structure is the same as the structure of the REPC_C model.

Model specification

The suite of generic GFM models are as shown in Figure 1, Figure 2, and Figure 3 for droop based, VSM based, and dVOC based grid forming structures respectively. In these figures, variables in blue color indicate input variables from the network to the control structure, orange color indicates output variables from the control structure to the network, green color indicates variables that can pass between different models, purple color indicates input reference values, and red color indicates state variables. All other variables are either local variables or control gains/flag settings. The *xy* reference frame is the real – imaginary coordinate frame of the network while the *dq* reference frame is the coordinate frame of the control. The relative angle between these reference frames is denoted by the control variable θ_{inv}.

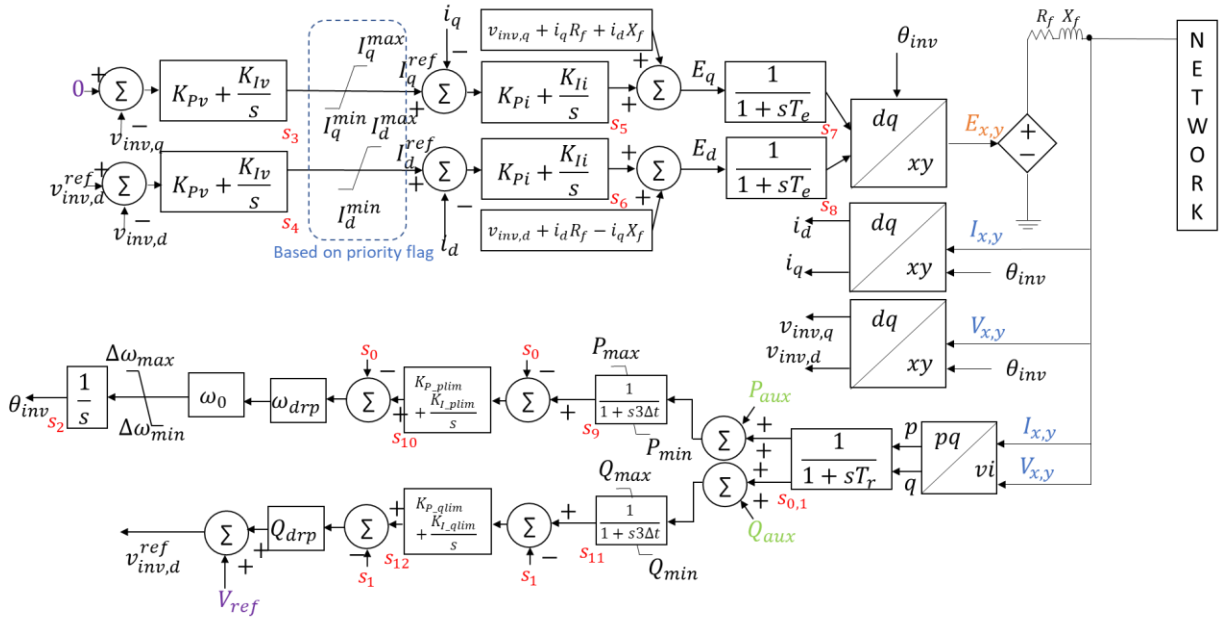

Figure 1: Generic grid forming model for droop based GFM

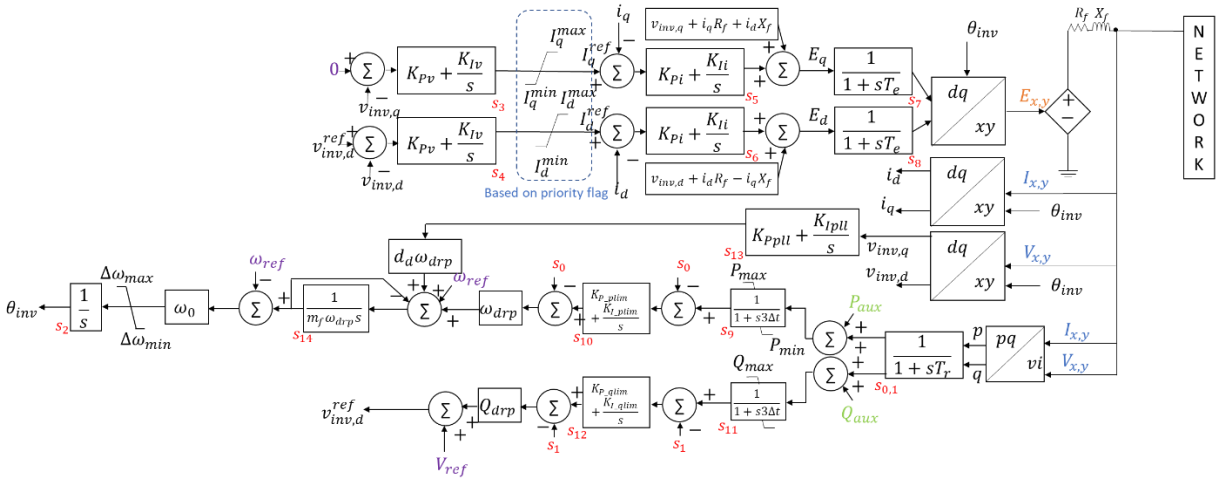

Figure 2: Generic grid forming model for VSM based GFM

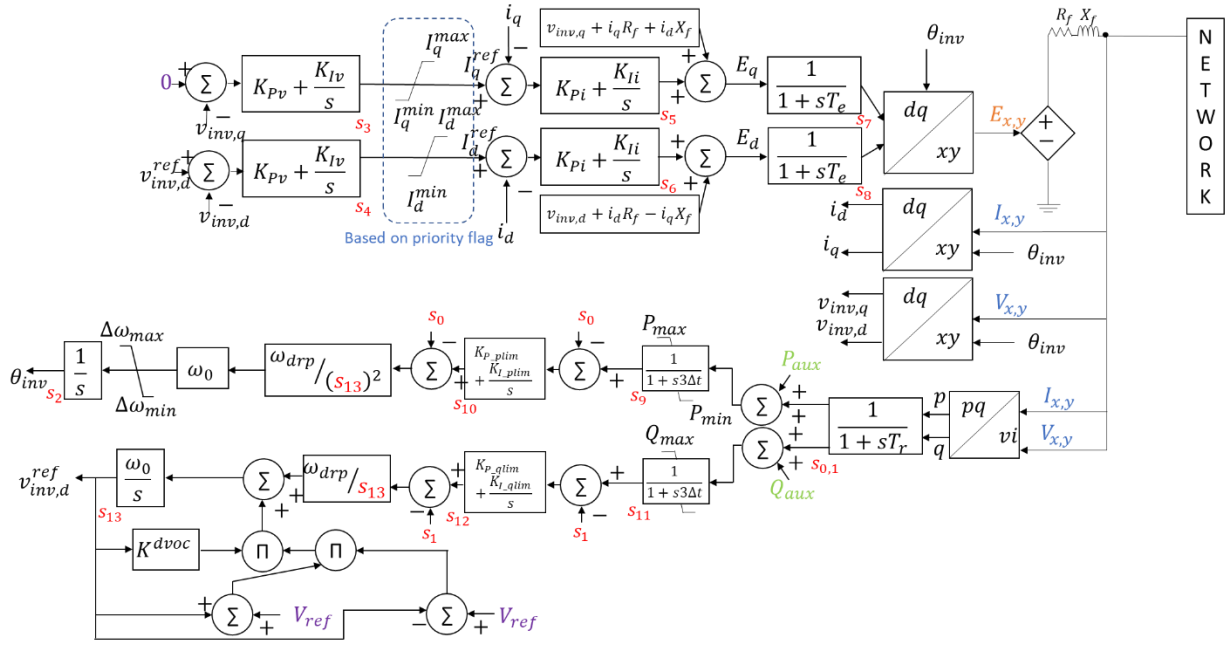

Figure 3: Generic grid forming model dVOC based GFM

Due to the generalized nature of the suite of models, many control gains and parameters shown in the figures are common across all three grid forming structures as tabulated in Table 1. For the VSM based generic model, two additional state variables are included to represent an additional measurement PLL and first order time constant. The additional four parameter specific only to the VSM based generic model are tabulated in Table 2.

Table 1: Parameters common across all three generic GFM models

Parameter	Description	Units	Default Value
MVA rating	IBR rating	MVA	100.0
R_f	Filter resistance	pu on MVA rating	0.0015
X_f	Filter reactance	pu on MVA rating	0.15
V_{dip}	State freeze threshold	pu	0.8
T_{frz}	Time to keep state frozen	s	0.5
I_{max}	Maximum current magnitude	pu	1.2
PQflag	Current priority	-	0 – P priority
			1 – Q priority
ω_0	Nominal angular frequency	rad/s	376.99
$\Delta\omega_{max}$	Maximum value of frequency deviation	rad/s	75.0
$\Delta\omega_{min}$	Minimum value of frequency deviation	rad/s	-75.0
ω_{drp}	Frequency droop percent	-	0.033
Q_{drp}	Voltage droop percent	-	0.045
T_r	Transducer time constant	s	0.005
T_e	Output state time constant	s	0.005
K_{Pi}	Current control proportional gain	-	0.5
K_{Ii}	Current control integral gain	-	20.0
K_{Pv}	Voltage control proportional gain	-	3.0
K_{Iv}	Voltage control integral gain	-	10.0
P_{max}	Maximum active power	pu on MVA rating	1.0
P_{min}	Minimum active power	pu on MVA rating	-1.0
K_{P_plim}	Proportional gain for P limits	-	5.0
K_{I_plim}	Integral gain for P limits	-	30.0
Q_{max}	Maximum reactive power	pu on MVA rating	1.0
Q_{min}	Minimum reactive power	pu on MVA rating	-1.0
K_{P_qlim}	Proportional gain for Q limits	-	0.1
K_{I_qlim}	Integral gain for Q limits	-	1.5

Table 2: Parameters specific to the VSM based GFM model

Parameter	Description	Units	Default Value
m_f	VSM inertia constant	-	0.15
d_d	VSM damping factor	-	0.11
K_{Ppll}	PLL proportional gain	-	20.0
K_{Ipll}	PLL integral gain	-	700.0

Finally, in the dVOC based generic model, one additional parameter K^{dvoc} is required in order to bring about sufficient voltage control. The value of this parameter is set based on equation (1).

$$\frac{K^{dvoc}}{\omega_{drp}} = \frac{4 * 100^4}{100^4 - \left(2 * \left(100 - 100 * Q_{drp}\right)^2 - 100^2\right)^2} \quad (1)$$

Here, parameters ω_{drp} and Q_{drp} are the values of droop, however not expressed in percent. For example, an ω_{drp} of 5% will be represented as 0.05. Additionally, the values of 100 in the equation do not imply MVA base of the inverter. In the model, all input reference values (purple colored variables) are specified in per unit on the MVA, kV rating, and nominal frequency of the IBR device. Further, input variables (blue colored variables) and output variables (orange colored variables) are also in per unit on the rating of the IBR device. It is expected that each software environment will handle the corresponding per unit conversions between the device and the network. Additionally, the network interface is modeled as a voltage source in a manner which is like the REGC_C model [8]. Due to the voltage source nature of the interface, there could also be a need to ensure current limits are maintained during a fault. This can require an algebraic iteration with the network solution at each time step during the fault. The method adopted in the REGC_C model and explained in detail in [8] [9] is also adopted in this model. Additionally, if needed, a shunt capacitor filter can be added on the grid side of X_f and its associated equations can be used in the determination of I_d^{ref} and I_q^{ref}.

The model also has the capability to receive signals P_{aux} and Q_{aux} from auxiliary control modules such as power oscillation dampers, automatic generation control blocks, plant controllers, etc. Additionally, when terminal voltage magnitude (i.e., $\sqrt{v_{inv,d}^2 + v_{inv,q}^2}$) falls below the freeze threshold V_{dip}, states $s_0, s_3, s_4, s_{10}, s_{11}$ are frozen in all three models along with state s_9 in the VSM based model. Additionally, similar to the REPC_C model, states s_{10}, s_{11} remain frozen for time T_{frz} seconds after the voltage recovers above the freeze threshold.

Commentary on use of inner current control loop

An inner current control loop is utilized to control the output current of the inverter and limit its value to a desired range of values, which are based on the inverter ratings. The control loop takes as its reference a desired output current of the inverter and uses it to compute voltage setpoints for the three-phase inverter. This results in the inverter operating as a signal-controlled voltage source. Such a grid forming control structure is often referred to as a multi-loop grid forming method.

Benchmarking of positive sequence generic model dynamic behavior against generic EMT model

The working of the proposed suite of generic GFM positive sequence models has been benchmarked against a corresponding model developed in EMT domain. The positive sequence models have been developed in GE-PSLF™ while the EMT models have been developed in PSCAD. EMT domain simulations are carried out at a time step of 5μs while positive sequence simulations are carried out a time step of 1ms.

To benchmark the model behavior, first a single inverter connected to an equivalent voltage source is considered. The setup of the network is as shown in Figure 4. At the start of the simulation the inverter is dispatched with $P_{ref} = 800MW$ and $V_{ref} = 1.035pu$ along with $P_{load} = 900MW$ and $Q_{load} = 210Mvar$. Since the dispatch of the IBR is lower than the total load, the surplus power is provided by the equivalent voltage source. At *t=5.0s* the breaker connecting the equivalent source to the rest of the circuit is opened thereby creating a 100% inverter network. Following this at *t=10.0s* a solid to ground three phase fault is applied at the POI.

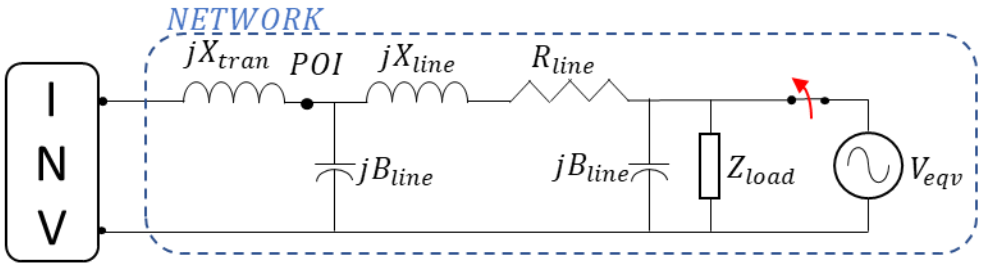

Figure 4: Single inverter-load-equivalent voltage source network to benchmark positive sequence model behavior

A comparison of the response in EMT domain across all four grid forming modes is shown in Figure 5 while a comparison of the response across all four grid forming models in positive sequence domain is shown in Figure 6. From both figures the similarity of the responses can be observed.

A one-to-one comparison of the behavior of the dVOC GFM model across both EMT domain and positive sequence domain is shown in Figure 7. When the equivalent source is disconnected,

initially there is a deficit in generation in the network as the IBR resource was dispatched at 800 MW. The deficit in generation both from active and reactive power results in voltage and frequency dropping. Subsequently, in all grid forming models, frequency and voltage is controlled with an increase in active power and reactive power output. The response for a subsequent three phase solid to ground fault is also shown. It is seen that across all grid forming models, both in EMT domain or positive sequence domain, the response of the suite of generic models is similar and consistent with seamless translation of parameter values.

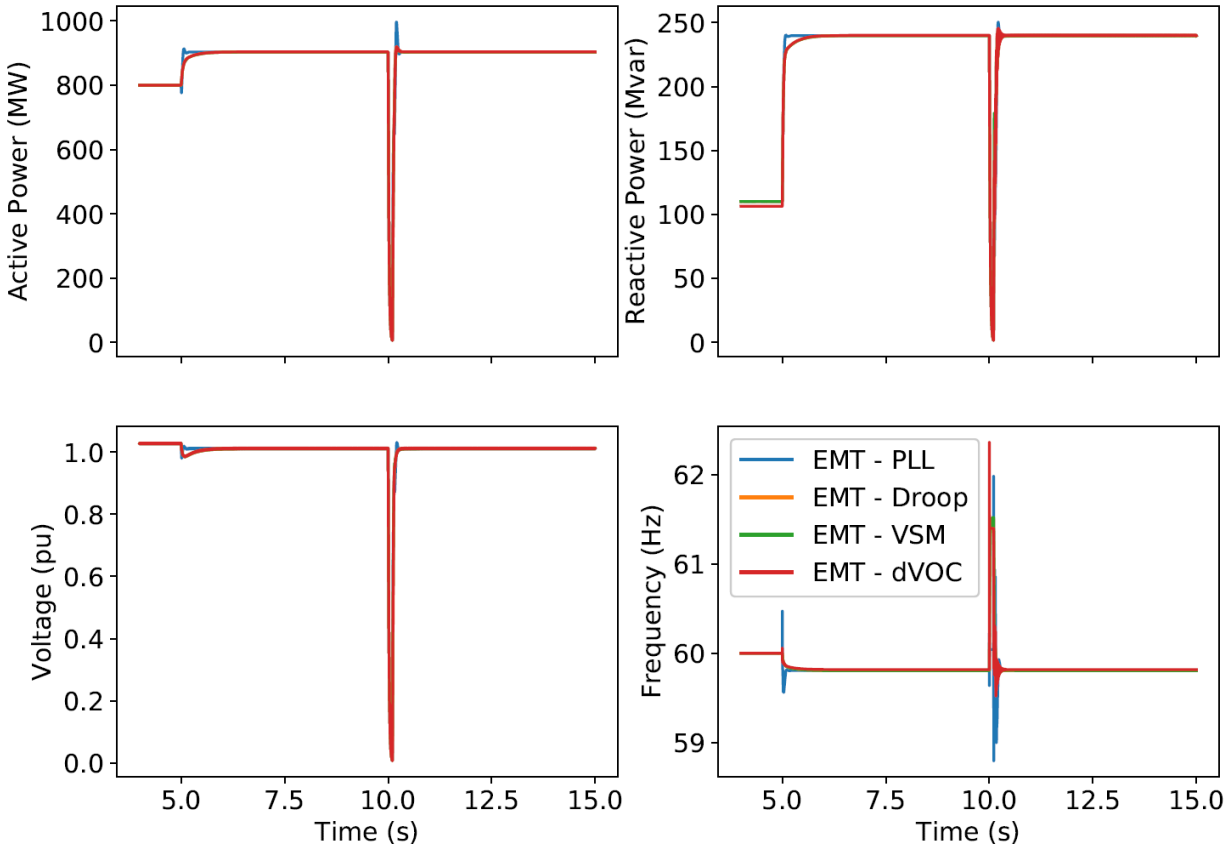

Figure 5: Comparison of EMT time domain response of the generic model in different GFM modes

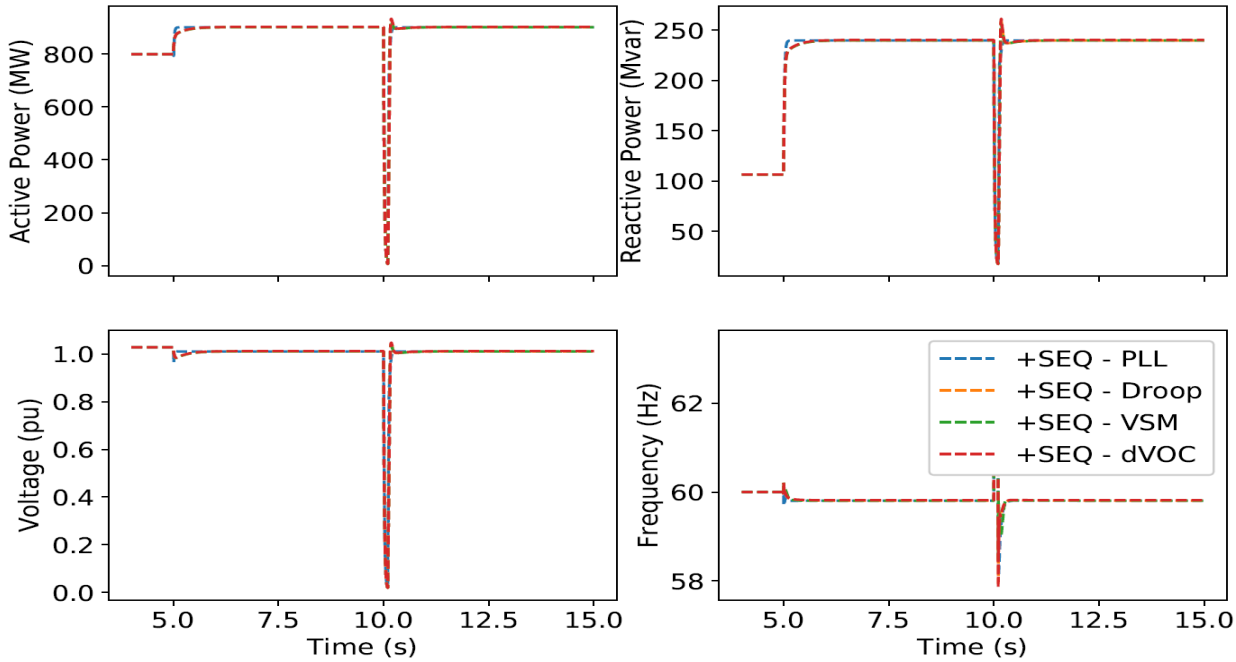

Figure 6: Comparison of positive sequence time domain response of the generic model in different GFM modes

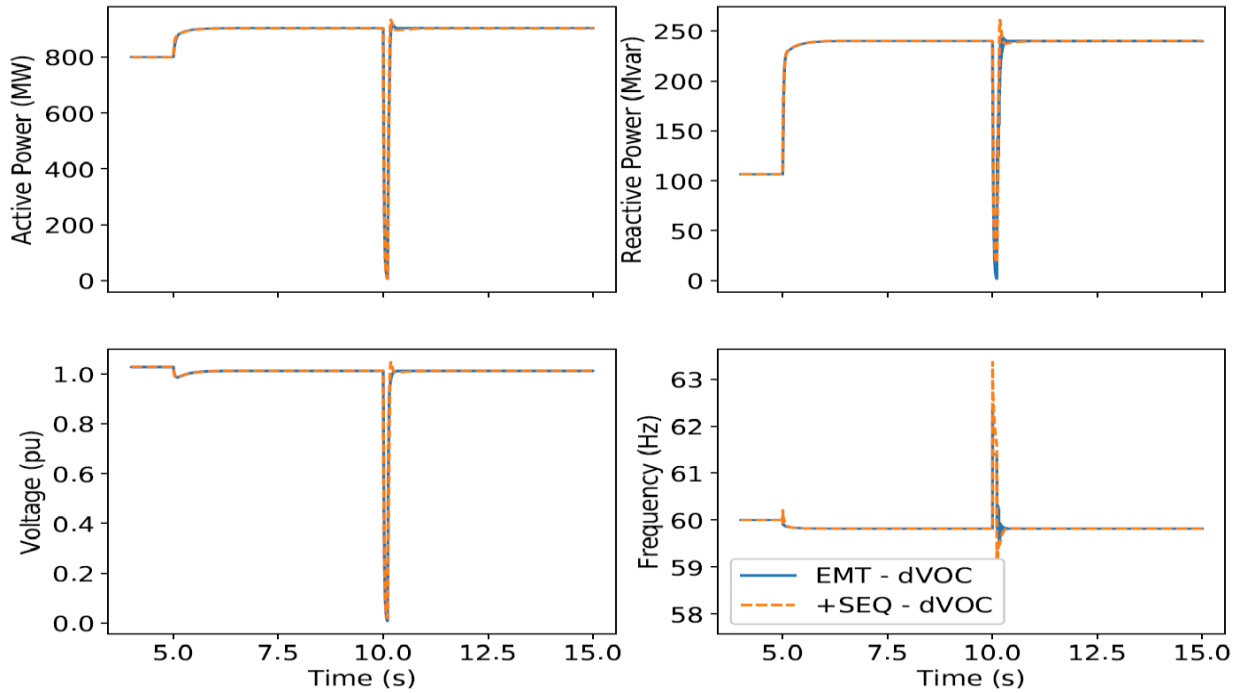

Figure 7: Comparison of EMT domain and positive sequence time domain response of the generic model in dVOC GFM mode

To extend the comparison to a multi-inverter resource system with different control types, the IEEE 14 bus benchmark system topology is used with a few modifications as shown in Figure 8. The response across both positive sequence domain and EMT domain to two consecutive load events at Bus 14 is shown in Figure 9. The comparison of response to multiple line outages followed by two consecutive three phase to ground solid faults is shown in Figure 10.

Both comparison results showcase the fidelity and robustness of the proposed suite of generic positive sequence models in being able to replicate the dynamic behavior of the grid forming devices.

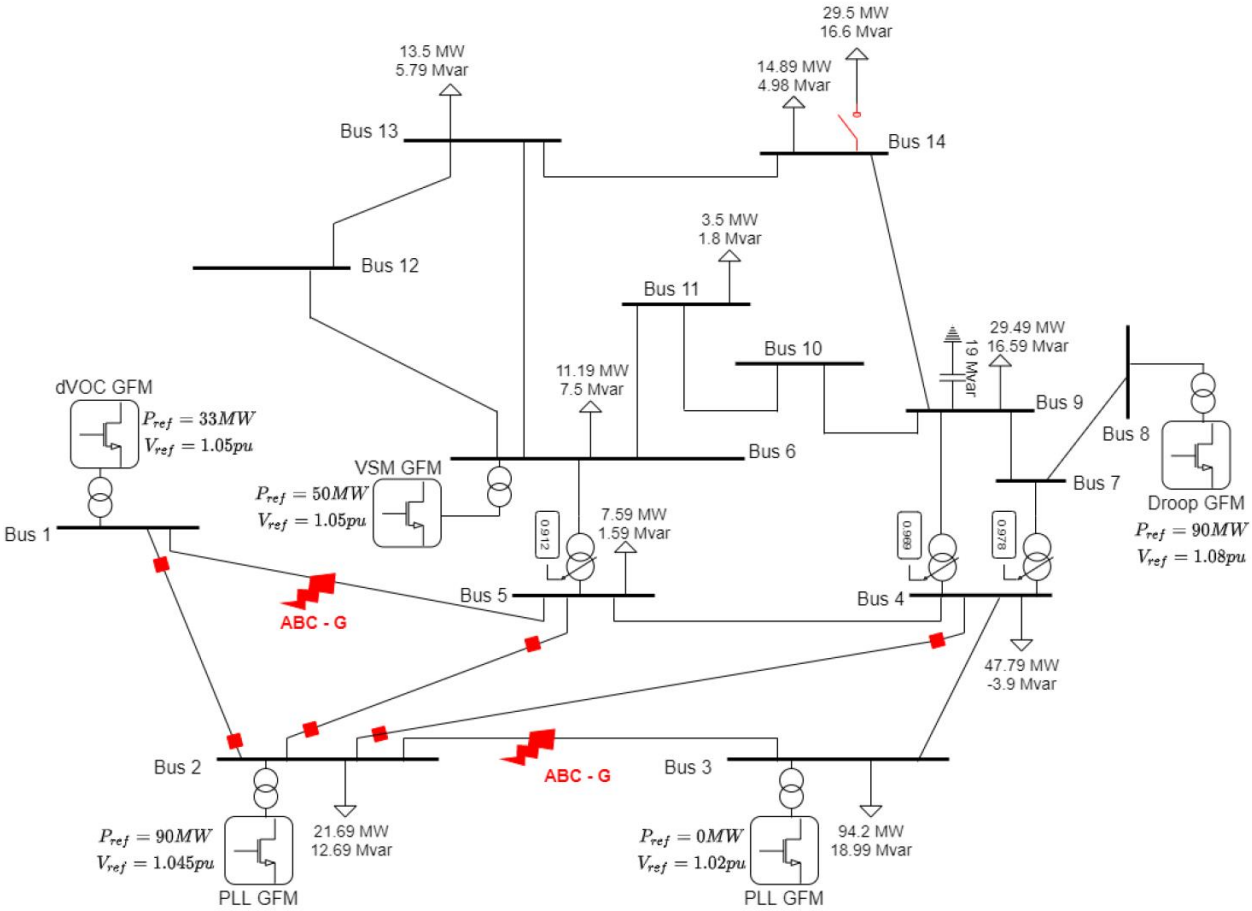

Figure 8: IEEE 14 bus benchmark system topology to benchmark model behavior with multiple IBR sources

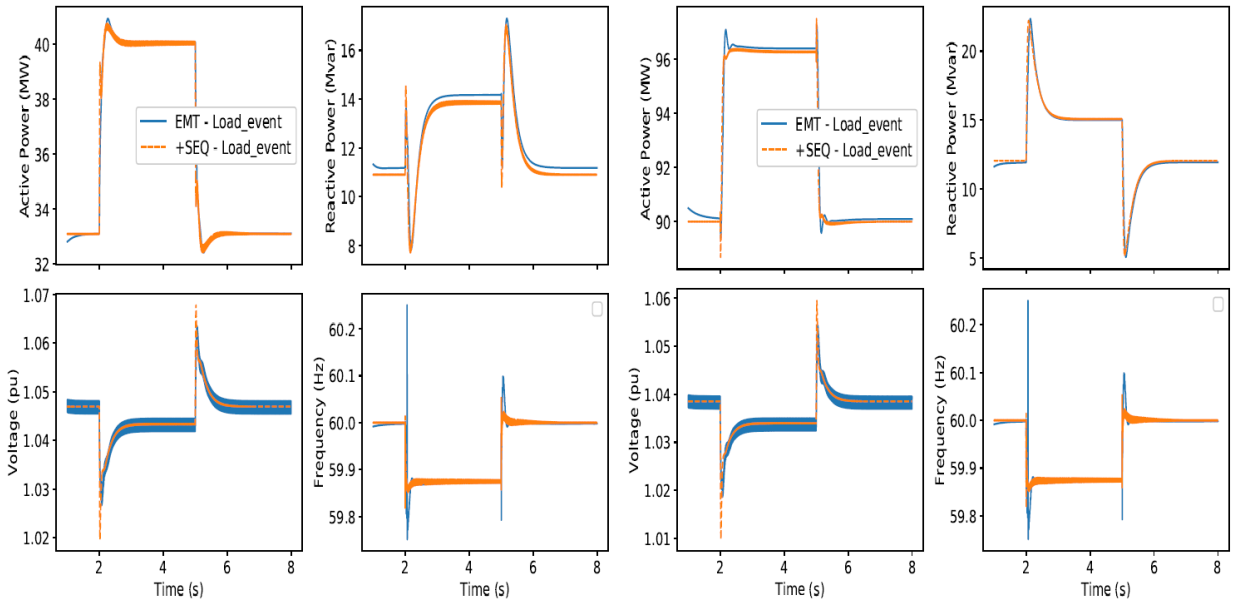

Figure 9: Behavior of IBR at bus 1 (left) and IBR at bus 2 (right) in response to two consecutive load events

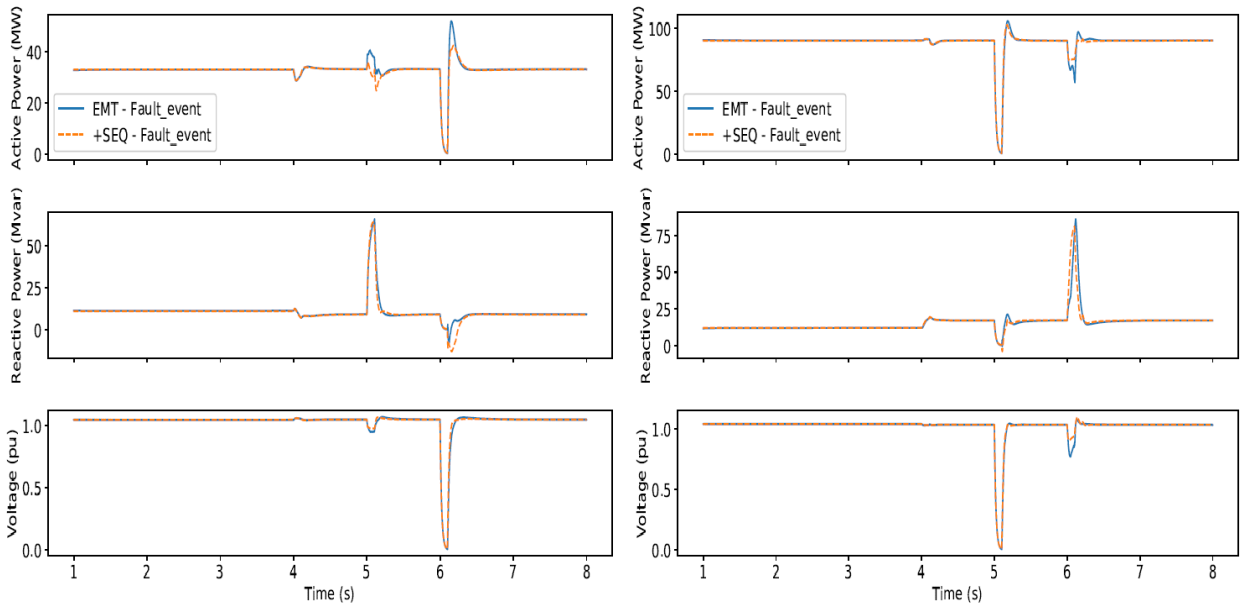

Figure 10: Behavior of IBR at bus 1 (left) and IBR at bus 2 (right) in response to multiple line outages followed by consecutive three phase to ground solid faults

Benchmarking generic positive sequence model response against original equipment manufacturer (OEM) black box EMT model

To further verify the behavior of the generic GFM positive sequence model for non-black start scenarios (as positive sequence simulations are not expected to be carried out for black start studies), the response of the generic model in PLL mode is compared against an OEM black box EMT model for a system islanding event. The reason for using the PLL mode here in this analysis is because the OEM model uses a combination of grid following control structure along with a virtual machine mode to bring about grid forming dynamics [10] both during a system interconnected operation and during subsequent islanded operation. It is again noted that in this scenario, a black start setup is not considered. The dynamic response for a disconnection of the system equivalent (resulting in a 100% IBR network) is shown in Figure 11.

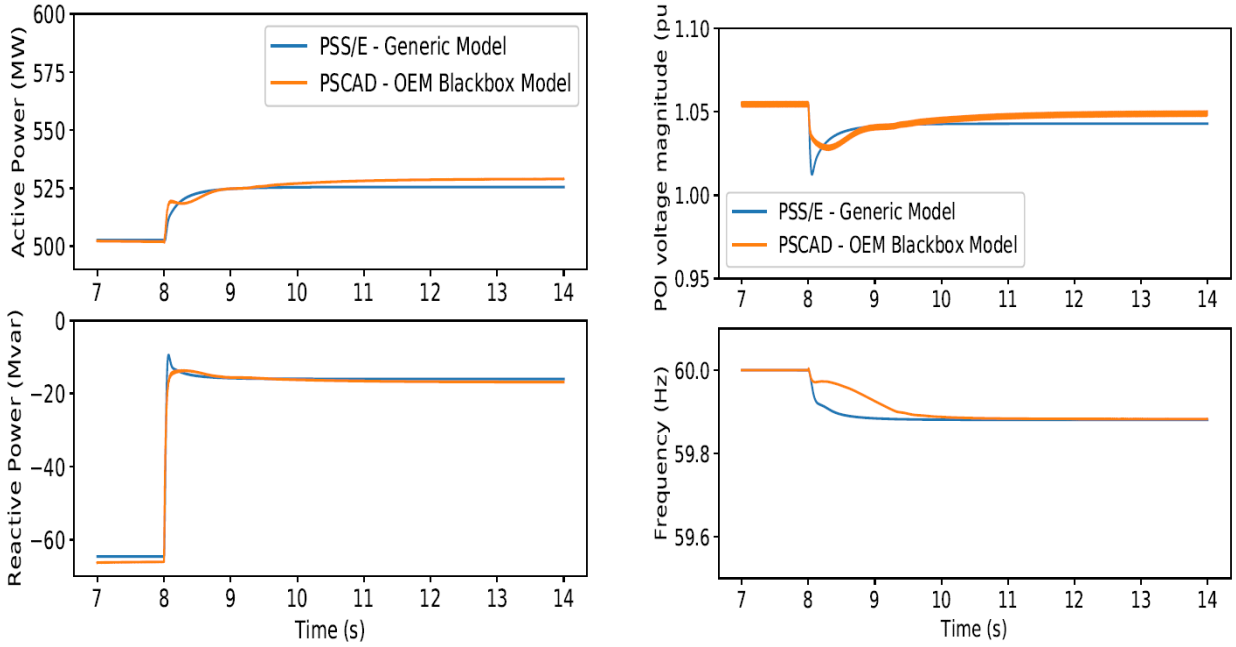

Figure 11: Dynamic response of positive sequence generic model behavior in PLL mode compared against OEM black box EMT model for system islanding event

The comparison of model behavior across both simulation domains, and a comparison of a generic positive sequence model with an OEM black box EMT model provides encouraging results regarding the validity of the suite of generic models. It is acknowledged that continuous validation studies with OEM models is to be carried out to keep the generic models up-to-date. However, with this suite of generic models, transmission planners can begin to evaluate the behavior of grid forming IBR devices in their networks.

Numerical robustness in practical power system base cases

The numerical robustness of the suite of models in practical bases cases has been verified and previously presented [11] [12] and is documented in [13]. Here, two practical cases have been considered: (i) a portion of the Eastern Interconnection converted into a 100% IBR network with few fictitious modifications, and (ii) a small island system.

To further evaluate the robustness of the suite of models, a large WECC system study was carried out. In this effort, an entire area of the WECC system was converted to a 100% IBR network. In the base case, this area has a mix of synchronous machine models and IBR models. In the base case 70% (by rating) of the online generation in the area are represented by synchronous machine models. To evaluate the robustness of the proposed suite of generic GFM models, all synchronous machines in the area were replaced with this suite of generic models, with equal rating/headroom. This results in a 100% IBR area with a mix of GFM and grid following IBRs in the same area. For the GFM resources, all four control methods were utilized and were assigned in a random fashion.

The event applied is the trip of 60% of the lines that connect this area to the rest of the interconnection. This results in reduction of the short circuit strength of the area in which the IBRs are connected. The trajectory of voltage and frequency as observed on a transmission bus at the area boundary is shown in Figure 12 and Figure 13 respectively. The blue curve corresponds to the base case (with synchronous machines in the area) while the red curve corresponds to the scenario with all synchronous machines in the area replaced with the suite of generic GFM models. With the reduction in short circuit strength, and the change in flow of power due to trip of the interconnecting tie lines, in the base case, the synchronous machines are unable to survive due to reduction of damping torque. However, with the GFM resources, since there are no mechanical time constants involved, the system can settle to an acceptable value of voltage with no deviation in frequency.

In both simulations, no numerical robustness issues were observed. This study showcases the ability to successfully use multiple instances of the same generic GFM model in a base case as large as the WECC base case.

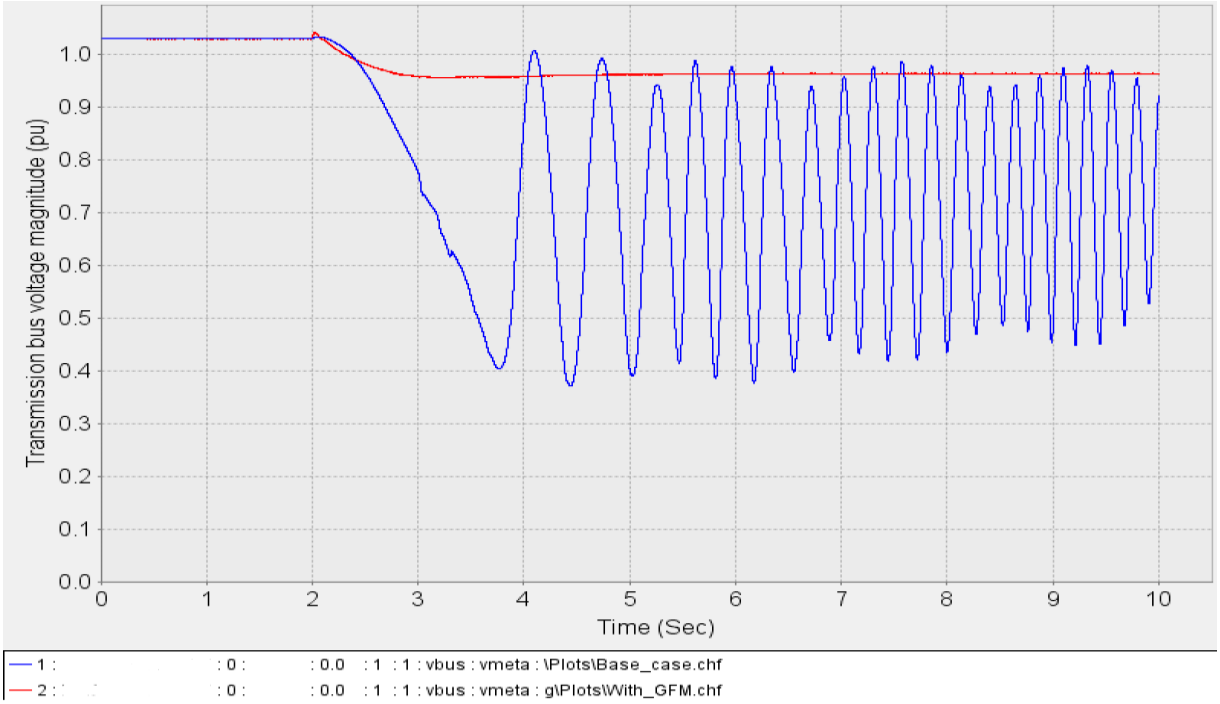

Figure 12: Voltage magnitude at transmission bus at the boundary of an area for an event disconnecting 60% of tie lines of the area (blue curve is base case with synchronous machines, red curve is with the suite of generic GFM models)

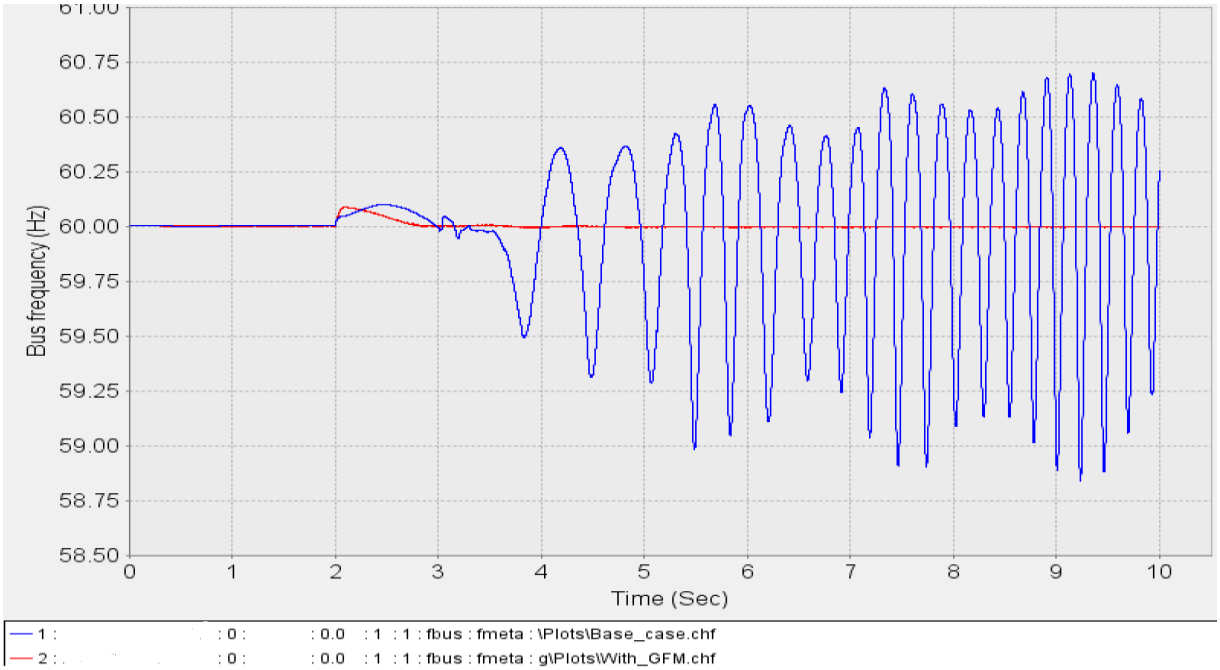

Figure 13: Bus frequency at transmission bus at the boundary of an area for an event disconnecting 60% of tie lines of the area (blue curve is base case with synchronous machines, red curve is with the suite of generic GFM models)

Acknowledgements
The development of this generic GFM model and its performance validation was supported, in part, by the U.S. Department of Energy, Solar Energy Technologies Office under Award Number DE-EE0009025 *A Scalable Control Architecture for 100% PV Penetration with Grid Forming Inverters* and, in part, by EPRI's Research Program 173: Bulk System Integration of Renewables and Distributed Energy Resources.

References

[1] B. Johnson, T. Roberts, O. Ajala, A. D. Dominguez-Garcia, S. Dhople, D. Ramasubramanian, A. Tuohy, D. Divan and B. Kroposki, "A Generic Primary-control Model for Grid-forming Inverters: Towards Interoperable Operation & Control," in *2022 55th Hawaii International Conference on System Sciences (HICSS)*, Maui, HI, USA, 2022.

[2] O. Ajala, N. Baeckeland, S. Dhople and A. D. Dominguez-Garcia, "Uncovering the Kuramoto Model from Full-order Models of Grid-forming Inverter-based Power Networks," in *IEEE Control and Decision Conference*, 2021.

[3] D. Ramasubramanian, "Differentiating between plant level and inverter level voltage control to bring about operation of 100% inverter-based resource grids," *Electric Power Systems Research,* vol. 205, no. 107739, 2022.

[4] D. Ramasubramanian and E. Farantatos, "Representation of Grid Forming Virtual Oscillator Controller Dynamics with WECC Generic Models," in *2021 IEEE PES General Meeting*, Washington D.C., USA, 2021.

[5] D. Ramasubramanian, P. Pourbeik, E. Farantatos and A. Gaikwad, "Simulation of 100% Inverter-Based Resource Grids With Positive Sequence Modeling," *IEEE Electrification Magazine,* vol. 9, no. 2, pp. 62-71, 2021.

[6] Electric Power Research Institute, "EMT and Positive Sequence Domain Model of Grid Forming PV Plant (GFM-PV)," EPRI, Palo Alto, CA, 2021, 3002021787.

[7] D. Ramasubramanian, "Memo on Proposal for Generic GFM Model," December 2021. [Online]. Available: https://www.wecc.org/_layouts/15/WopiFrame.aspx?sourcedoc=/Administrative/Memo%20on%20Proposal%20for%20Generic%20GFM%20Model_v2.pdf&action=default&DefaultItemOpen=1. [Accessed January 2022].

[8] D. Ramasubramanian, W. Wang, P. Pourbeik, E. Farantatos, A. Gaikwad, S. Soni and V. Chadliev, "Positive Sequence Voltage Source Converter Mathematical Model for Use in Low Short Circuit Systems," *IET Generation, Transmission & Distribution,* vol. 14, no. 1, pp. 87-97, 2020.

[9] D. Ramasubramanian, A. Gaikwad, E. Farantatos and P. Pourbeik, "A Method of Implementation of Current Limits in REGC_B and REGC_C," 4 March 2019. [Online]. Available: https://www.wecc.org/Reliability/Memo%20on%20EPRI's%20method%20for%20implementation%20of%20current%20limit%20logic%20in%20REGC_B_C.pdf. [Accessed 3 November 2021].

[10] North American Electric Reliability Corporation, "Reliability Guideline: Performance, Modeling, and Simulations of BPS-Connected Battery Energy Storage Systems and Hybrid Power Plants," NERC, Atlanta, GA, 2021.

[11] D. Ramasubramanian, "Simulation of 100% IBR grids with positive sequence modeling," August 2021. [Online]. Available: https://www.wecc.org/_layouts/15/WopiFrame.aspx?sourcedoc=/Administrative/Ramasubramanian%20-%20Simulation%20of%20100%20IBR%20Grids%20with%20Positive%20Sequence%20Modeling.pdf&action=default&DefaultItemOpen=1. [Accessed November 2021].

[12] D. Ramasubramanian, "Modeling of grid forming (GFM) IBR and frequency response in a 100% IBR Grid," October 2021. [Online]. Available: https://www.wecc.org/_layouts/15/WopiFrame.aspx?sourcedoc=/Administrative/WECC%20Grid%20Forming%20Inverter%20Based%20Resources%20.1.pdf&action=default&DefaultItemOpen=1. [Accessed November 2021].

[13] Electric Power Research Institute, "Grid Forming Inverters for Increase in Inverter Based Resource Percentage," EPRI, Palo Alto, CA, 2021, 3002020786.